

Large-Area Photoconductive Terahertz Detectors

S. Winnerl¹⁾, F. Peter¹⁾, S. Nitsche¹⁾, A. Dreyhaupt¹⁾, O. Drachenko¹⁾, H. Schneider¹⁾, M. Helm¹⁾
and K. Köhler²⁾

¹⁾Institute of Ion Beam Physics and Materials Research, Forschungszentrum Dresden-Rossendorf,
P.O. Box 510119, D-01314 Dresden, Germany

²⁾Fraunhofer-Institute for Applied Solid State Physics, 79108 Freiburg, Germany
e-mail: s.winnerl@fzd.de

Abstract

We present a novel non-resonant photoconductive antenna for coherent detection of THz radiation. The antenna consists of an interdigitated electrode structure, where every other electrode gap is covered by a second metallization layer. Different substrate materials with different carrier lifetimes are compared. These antennas are easy to use and offer a high degree of freedom with respect to the focusing of both the THz and the gating beam.

Introduction

Single cycle terahertz radiation was first studied using photoconductive emitter and detector antennas [1]. Electro-optic sampling [2] then has been often used for detection, mainly due to its large THz bandwidth and quantitative detection properties [3]. Detection antennas have been developed and optimized in various directions. By using 15 fs laser pulses for gating dipole antennas on low-temperature-grown (LT) GaAs a bandwidth up to 20 THz was achieved [4]. Using a shaker technique for temporal differentiation of the THz waveforms the bandwidth was extended up to 60 THz [5]. Recently materials prepared by ion implantation were successfully used as alternatives for LT-GaAs [6, 7].

In this study we demonstrate THz detection with a scalable large area antenna, which has been used as an efficient THz emitter previously [8, 9]. LT-GaAs, N⁺ implanted GaAs and semi-insulating (SI) GaAs substrates are compared with respect to their detection properties.

Experimental

Our photoconductive antenna is an interdigitated electrode structure as shown in Fig. 1. Every other spacing between the gold fingers (electrode width 5 μm , spacing 5 μm) is covered by a second metallization, which is electrically isolated from the first one. If the structure is exposed to a THz field while an optical gating pulse is applied, the photo-generated electrons and holes induce a different electrical potential at electrode 1 and 2; thus a net photocurrent is flowing in the external circuit. In the absence of the second metallization layer (see upper part of Fig. 1), the photocurrent would vanish due to equal contributions of opposite polarity. The detection antenna has an active area of 1 mm² and is placed at a distance of 23 mm from a THz emission antenna. The active area of the emission antenna is 9 mm² and its electrode structure is similar as for the detection antenna. While the emitter antenna is based on SI-GaAs, different materials are used for the detection antennas. Sample 1 is LT-GaAs (layer thickness: 2 μm , growth temperature: 200 $^{\circ}\text{C}$, annealed at 600 $^{\circ}\text{C}$ in N₂ ambient for 10 min), sample 2 is GaAs implanted with N⁺ (dual energy implant, 0.4 MeV, dose $1 \times 10^{13} \text{ cm}^{-2}$ and 0.9 MeV, dose $3 \times 10^{13} \text{ cm}^{-2}$). This implantation results in a damage profile

extending to a depth of about 1.2 μm . Sample 3 is implanted similarly to sample 2, but subsequently annealed in N₂ ambient at 500 $^{\circ}\text{C}$ for 10 min. For comparison, sample 4 is processed on SI-GaAs.

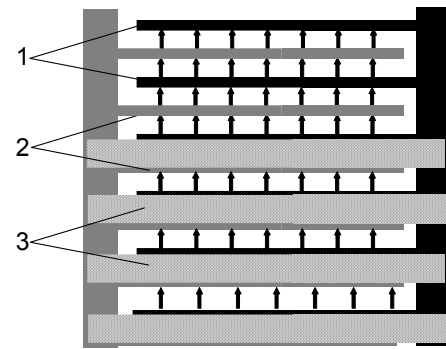


Fig. 1: Layout of the detector; 1) and 2) electrodes, 3) second metallization. The arrows indicate the photocurrent in the substrate.

Laser pulses (wavelength 786 nm, repetition rate 78 MHz, duration 50 fs) are used to excite the THz emitter and to gate the detection antenna. The spot size (FWHM) and average power of the near infrared radiation are 300 μm and 350 mW on the emitter and 400 μm and 70 mW on the detector antenna, respectively. The emitter is electrically driven by a rectangular bias voltage with amplitudes of $\pm 12.5 \text{ V}$ and a frequency of 5 kHz. The photocurrent of the detection antenna is amplified by a low-noise current amplifier and measured via lock-in detection (integration time constant 100 ms), where the bias voltage at the emitter serves as a reference.

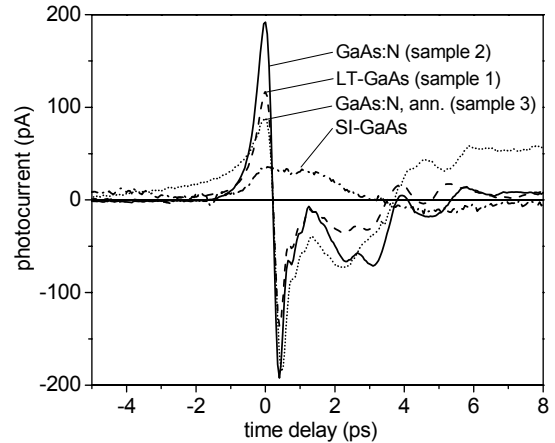


Fig. 2: Detected photocurrents for the antennas based on different substrate materials.

Results and Discussion

The photocurrents of the different samples are shown in Fig. 2. Clearly the SI-GaAs with a carrier lifetime of a few tens of ps yields much smaller signal amplitudes and temporally broadened signals compared to the materials with short carrier lifetimes. The broadened signal of the N^+ implanted and subsequently annealed sample compared to the as-implanted sample indicates that the annealing process results in an increased carrier lifetime. Long carrier lifetimes lead to an increase of the noise on the detector signal. Noise currents measured in the time interval (-10 ps, -5 ps) are compared in table 1. The as-implanted GaAs:N detector exhibits the strongest signal, however, its noise is two times larger than the noise of the LT-GaAs detector. The signal/noise ratios of these two detectors are comparable, while the materials with the longer carrier life times have much smaller values. The good figures for the signal/noise ratio for sample 1 and 2 demonstrate that this detector is well suited for detection of unfocused THz radiation. The large-area detector allows using high gating power (70 mW in this experiment) without strong saturation effects which are present in conventional antennas with active areas of few μm^2 [10].

Sample	Signal (p-p)	Noise (rms)	Signal/Noise
Sample 1	253 pA	0.1 pA	2530
Sample 2	384 pA	0.2 pA	1920
Sample 3	274 pA	0.6 pA	457
Sample 4	47 pA	1.0 pA	47

Table 1: Comparison of peak-peak signal, noise current (rms) and signal/noise ratio for the different detectors.

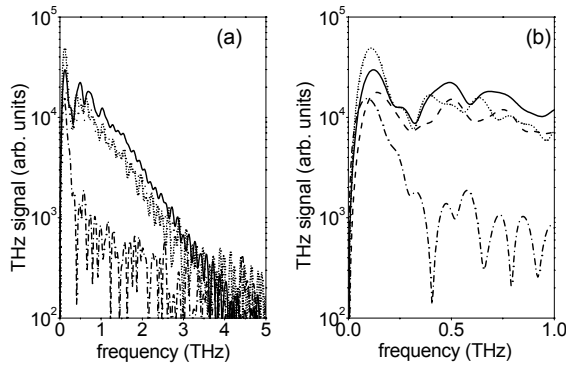


Fig. 3: Spectra for a larger (a) and smaller (b) frequency range. The different materials are sample 1 (dashed), sample 2 (solid), sample 3 (dotted) and sample 4 (dash-dotted).

The Fourier transforms of the photocurrent are plotted in Fig. 3. The spectra extend up to about 3 THz except for the SI-GaAs detector, which shows strongly reduced signals for frequencies above 0.3 THz. The pronounced structures on the spectra are due to reflections on the semiconductor surfaces and absorption by water vapor. The as-implanted GaAs:N detector provides the strongest signals in the frequency range from 0.5 THz – 3 THz. In this range spectra of the LT-GaAs emitter and the annealed implanted GaAs detector are very similar. For very low frequencies, namely between 50 and 200 GHz, the annealed GaAs:N detector provides stronger signals than the other detectors.

In conclusion we have demonstrated a detector concept which is suitable for the detection of THz radiation without the need of strong focusing. Since the detectors have a large area, they are easy to align and robust with respect to beam pointing fluctuations. Comparing different materials we obtained best results for LT-GaAs and N^+ implanted GaAs which was not annealed.

Acknowledgment

We thank A. Kolitsch for valuable discussions concerning the ion implantation. Part of this work has been supported by EuroMagNET under EU contract RII3-CT-2004-506239.

References

- [1] D.H. Auston, K.P. Cheung, and P.R. Smith, "Picosecond photoconducting Hertzian dipoles", *Appl. Phys. Lett.* vol. 45, 1984, pp. 284-286.
- [2] Q. Wu and X.-C. Zhang, "Ultrafast electro-optic field sensors", *Appl. Phys. Lett.* vol. 68, 1996, pp. 1604-1606.
- [3] A. Leitenstorfer, S. Hunsche, J. Shah, M.C. Nuss, and W.H. Knox, "Detectors and sources for ultrabroadband electro-optic sampling: Experiment and theory", *Appl. Phys. Lett.* vol. 74, 1999, pp. 1516-1518.
- [4] S. Kono, M. Tani, P. Gu, and K. Sakai, "Detection of up to 20 THz with a low-temperature-grown GaAs photoconductive antenna gated with 15 fs light pulses", *Appl. Phys. Lett.* vol. 77, 2000, 4104-4106.
- [5] S. Kono, M. Tani, and K. Sakai, "Coherent detection of mid-infrared radiation up to 60 THz with an LT-GaAs photoconductive antenna", *IEE Proc. Optoelectron.* vol. 149, 2002, pp. 105-109.
- [6] T.-A. Liu, M. Tani, M. Nakajima, M. Hangyo, K. Sakai, S. Nakashima, and C.-L. Pan, "Ultrabroadband terahertz field detection by proton-bombarded InP photoconductive antennas", *Opt. Express* vol. 12, 2004, pp. 2954-2959.
- [7] B. Salem, D. Morris, V. Aimez, J. Beauvais, and D. Houde, "Improved characteristics of a terahertz set-up built with an emitter and detector made on proton-bombarded GaAs photoconductive materials", *Semicond. Sci. Technol.* vol. 21, 2006, pp. 283-286.
- [8] A. Dreyhaupt, S. Winnerl, T. Dekorsy, and M. Helm, "High-intensity terahertz radiation from a microstructured large-area photoconductor", *Appl. Phys. Lett.* vol. 86, 2005, 121114.
- [9] A. Dreyhaupt, S. Winnerl, M. Helm, and T. Dekorsy, "Optimum excitation conditions for the generation of high-electric-field terahertz radiation from an oscillator-driven photoconductive device", *Opt. Lett.* vol. 31, 2006, pp. 1546-1548.
- [10] M. Suzuki and M. Tonouchi, "Fe-implanted InGaAs terahertz emitters for 1.56 μm wavelength excitation", *Appl. Phys. Lett.* vol. 86, 2005, 051104.